



Semnan University



Heat Transfer Correlation for Two Phase Flow in a Mixing Tank

Mansour Jahangiri*, Omid Delbari

Faculty of Chemical, Petroleum and Gas Eng., Semnan University, Semnan, 35131-19111, Iran.

PAPER INFO

Paper history:

Received: 2019-10-07

Revised: 2020-01-21

Accepted: 2020-02-01

Keywords:

Heat transfer;
OpenFoam;
Mixing Tank;
Nusselt number.

ABSTRACT

Mixing tanks equipped with mechanical stirrer are broadly applied in chemical and petrochemical industries, due to their variety of industrial process requirements. In this study, helical single blade mixer was designed applying CATIA and then mixing of fluid and solid particles, in a tank with this agitator was examined by OpenFOAM. For velocity distribution in the mixing tank, continuity, momentum equations, boundary conditions and coding were performed applying C++ language scripts in the software. The results of velocity distributions in three directions coordinates indicated that the efficiency of helical blade mainly correlated to axial and tangential flows. The radial flow has less important role in mixing operation. Moreover, solid particles concentration distribution were computed in the fluid phase. It was exhibited that the particles were distributed homogeneously in the tank. In addition, temperature distribution was obtained applying continuity, momentum and energy equations as well as utilizing necessary code and boundary conditions in the software. Consequently, a correlation for Nusselt number as a function of Re, Pr and Vi was acquired by using temperature profile and dimensional analysis. The results achieved are in good agreement with those available in literature.

DOI: 10.22075/jhmtr.2020.17712.1232

© 2020 Published by Semnan University Press. All rights reserved.

1. Introduction

Tanks equipped with mechanical stirrer are broadly applied in the chemical and petrochemical industries. The temperature of the fluid inside the reactor is one of the most important factors that need to control the output products. Therefore, in order to control the quality of products, it is necessary to explore the heat transfer in stirred tanks. The heat transfer rate of fluid in the mixing tank depends on the parameters such as tank design, mixer type, and process conditions. Moreover, the flow pattern in a stirred tank relies on the impeller type, physical properties of the fluid, geometrical characteristics of the tank, and propeller specifications [1-6]. Laboratory researches were demonstrated on hydrodynamic characteristics of fluids in the tanks with different forms of agitators [7-10]. Nowadays, the studies done by advanced numerical simulations are based on computational fluid dynamics (CFD) methods [11-15]. Also, in recent years, the numerical calculation of mixing in the stirred tank has attracted much attention. The rapid development and wide numerical techniques and application capabilities at the

moment can use very complex engineering techniques. Computational fluid dynamics is an essential tool in order to understand the mixing process in stirred tanks [15-17]. Jahangiri [18-22] acquired the velocity distribution of impeller in the mixing of viscoelastic fluids in the transition region applied laser Doppler anemometry. Liu [23] has investigated fluid flow with different impellers in mixing tanks applying CFD and compared finding with experimental values. Recently, Rosa and Júnior [24], were reviewed the heat transfer of non-Newtonian fluids in agitated tanks. An equation proposed by Coyle et al. [25] assumes that, for viscous fluids, heat transfer is by steady conduction through a static film near the vessel wall as follows:

$$h_j = k(c/2)^{-1} \quad (1)$$

h_j , k , and c are film heat transfer coefficient, thermal conductivity, and clearance, respectively.

Overall heat transfer rate Q is giving by

$$Q = h_j A (T_b - T_w) \quad (2)$$

Their study displayed that the heat transfer coefficient

*Corresponding Author: Mansour Jahangiri, Faculty of Chemical, Petroleum and Gas Eng., Semnan University, Semnan, 35131-19111, Iran. Email: mjahangiri@semnan.ac.ir

was affected by impeller speed.

Harriott [26] and Latinen [27] independently solved the one-dimensional transient heat conduction and proposed the following equation to describe the average heat transfer coefficient, h_j , for the scraped surface (based upon the temperature difference between the wall and the bulk fluid):

$$h_j = 2 \sqrt{\frac{C_p \rho k}{\pi t}} \quad (3)$$

The contact time, t , is equal to $1/Nn_b$, where n_b is the number of blades, and N is the rotational speed of the impeller. Thus:

$$h_j = 2 \sqrt{\frac{C_p \rho k N n_b}{\pi}} \quad (4)$$

Equation (4) may also be put in the dimensionless form:

$$\left(\frac{h_j T}{k}\right) = 1.1 \left(\frac{\rho N T^2}{\mu}\right)^{1/2} \left(\frac{C_p \mu}{k}\right)^{1/2} n_b^{1/2} \quad (5)$$

However, the simple penetration theory, Eq. (4), was found to overestimate laminar heat transfer data for close clearance mixers by as much as 700% [28]. Rautenbach and Bollenrath [28] modified the film penetration model of Harriott [26] proposed the following relationship for heat transfer to viscous materials at low Reynolds numbers:

$$Nu = 0.568 \left[\frac{\left(\frac{k}{\rho C_p}\right)}{C^2 N n_b} \right]^{-0.23} \left(\frac{c}{T}\right)^{-1} \quad (6)$$

In dimensional analysis, convective heat transfer data may be correlated in the following form:

$$Nu = \text{fn}(\text{Re}, \text{Pr}, \text{Vi}, \text{shape factors}) \quad (7)$$

Where Nu , Re , Pr , and Vi are Nusselt, Reynolds, Prandtl numbers, and viscosity ratio, respectively. The functional relationship between the variable in Eq. (7) is usually established from experimental work and have reported as [27-31] follows:

$$Nu = A \text{Re}^a \text{Pr}^b \text{Vi}^d (\text{shape factor})^\varepsilon \quad (8)$$

Negata et al. [32], presented the correlation for ribbons in the range $\text{Re} > 1000$ as

$$Nu = 0.37 \text{Re}^{2/3} \text{Pr}^{1/3} \text{Vi}^{0.14} \quad (9)$$

It was reported that impeller geometry had little effect on heat transfer as well.

Table 1 illustrates some experimentally based heat transfer correlations [33]. Critical impeller speed, N_c , is a function of fluid properties and system geometry, it may be written as follows:

$$N_c = \text{fn}(\rho, \mu, C_p, k, C, p, n_b, \text{other shape factor}) \quad (10)$$

Consequently, by dimensional analysis, it is possible to display that:

$$\frac{\rho N_c D^2}{\mu} = \text{fn} \left[\left(\frac{\mu C_p}{k}\right) \left(\frac{c}{D}\right) \left(\frac{p}{D}\right) (n_b) \dots \right] \quad (11)$$

The literature review indicates that few works were inspected for the agitating and heat transfer for helical ribbon impeller in two-phase flow in the mixing tank. Despite that, two-phase heat transfer in conventional tubes

and channels is an ongoing research topic, especially for the refrigeration and air-conditioning fields [34]. Therefore, this study explores the heat transfer of the jacketed tank in which the hot fluid is in the jacket. The OpenFOAM was employed for simulation. The coding was contemplated taking into account the effect of interaction between solid particles, solid-fluid particle, continuity equation, energy equation, momentum equation. The solution approach in the present work was chosen by multiple reference frames (MRF) method [4,9].

2. Model Development

2.1. OpenFOAM

The OpenFOAM can be employed for a wider range of physical Phenomena such as compressible and incompressible flows, two-phase flow (gas-particle, fluid-fluid), flow in porous materials, gas dynamics, combustion, turbomachinery, etc. The main gift of OpenFOAM is resulting from the clever use of the capabilities of the C++ scripting language. This is an object-oriented scripting language. In addition, encountering some pre-written solvers for different problems, the OpenFOAM program employs the skills of the language C++, regular structure of classes, libraries, and in general provided objects enable the development and customization of the code in order to solve any particular problems.

2.2. Problem assumptions

The steady-state flow mixing was deliberated in 3-D directions. The model consists of two-phase without reactions. Therefore, the governing equations are as follows.

2.3. Governing equations

The governing equations are as follows:

2.3.1. Particle phase

The motion of particles in the fluid is assumed as the Lagrangian approach, in which the system of differential equations is pondered for calculation of particles displacement and changes of velocity component. On that account, paying attention to all forces that were affected on the particles is required. Moreover, the motion of spherical particles in a fluid may be described by the following relationships:

$$\frac{d\vec{X}_p}{dt} = \vec{V}_p \quad (12)$$

$$m_p \frac{d\vec{V}_p}{dt} = \Sigma \vec{F} \quad (13)$$

Where X_p and V_p are the local coordinate and particles velocity, respectively. The right side of equation (13) is the summation of forces acting on the particle. Depending on flow type and particle size, different forces may be lead to a problem. Forces that are regulator the motion of the particles may be divided into three kinds:

Table 1. Heat transfer correlations for helical ribbons (single-phase) [33-37].

D	T	p/D	w/D	c/T	n _b	Rerange	Correlation
0.28	0.3	0.5	0.18	0.033	1	8-10-5	$Nu = 0.633Re^{1/2}Pr^{1/3}Vi^{0.18}$
0.240	0.3	1	0.12	0.100	2	0.1-Rec	
0.264		1	0.108	0.060	2	Rec=39T/(T-D)	$Nu = 1.75Re^{1/3}Pr^{1/3}Vi^{0.2} \left(\frac{T-D}{D}\right)^{-1/3}$
0.280		1	0.102	0.033	2		
0.284		1	0.10	0.027	2	0.8<D/T<0.97	
0.290		1	0.98	0.017	2	Rec-106	$Nu = 0.52Re^{2/3}Pr^{1/3}Vi^{0.14}$
0.264	0.3	1	0.108	+Scraper	2	0.1-Rec	$Nu = 5.4Re^{1/3}Pr^{1/3}Vi^{0.2}$
0.148	0.155	1	0.11	0.023	2	5-50	$Nu = 2.0Re^{1/3}Pr^{1/3}Vi^{0.14}$
					4	50-500	$Nu = 1.0Re^{1/2}Pr^{1/3}Vi^{0.14}$
						500-8 *104	$Nu = 0.35Re^{2/3}Pr^{1/3}Vi^{0.14}$

1. The forces which are between the levels contact the particles with the fluid act.
2. Forces that arise as the outcome of the interaction between particles.
3. Forces applied to an external field.

The first kind is contained of forces such as drag, saffman, pressure gradient, buoyancy. The second type comprises van der Waals forces, electrostatic and force of collisions between particles in the four-sided correlation are investigated. Forces such as gravity and magnetic forces are the third form. The forces applied to the particles defined as:

2.3.1.1. Drag force

In fluid-particle systems, drag is the most important force applied to the particles and computed by the equation below.

$$\vec{F}_D = \frac{3}{4} m_p \mu_f C_D / \rho_p \sqrt{d} \quad (14)$$

2.3.1.2. Pressure gradient

The local pressure gradient in flow makes an additional force in the reversed path of the pressure gradient. This force for a spherical particle is deliberated as follows:

$$\vec{F}_p = -\frac{\pi d^3}{6} \nabla P \quad (15)$$

That

$$\vec{F}_p = m_p \frac{\rho_f}{\rho_p} \times \frac{Du_f}{Dt} \quad (16)$$

2.3.1.3. The weight and buoyancy

The gravity is effective in a solid-fluid system like buoyancy force. The total gravity effects are the sum of weight and buoyancy forces that is achieved as below:

$$\vec{F}_{gr} = (\rho_p - \rho_f) \frac{\pi d^3}{6} \vec{g} = m_p g \left(1 - \frac{\rho_f}{\rho_p}\right) \quad (17)$$

2.3.1.4. The force Saffman lifting

In areas where the shear stress is high such as near the wall, the velocity gradient is large. In this case, a force can exist in the direction perpendicular to the flow. This force is known as Saffman that is given as below

$$\vec{F}_s = C_s \frac{m_p d \rho_f}{2 \rho_p} \left((U_f - U_p) \times \omega \right) \quad (18)$$

2.3.2. Fluid phase

In the Euler-Lagrange method, the fluid phase can be simulated with the Eulerian view. At steady state in Cartesian coordinates the governing equations of fluid include the equations of continuity, momentum, and energy as follows:

Continuity equation:

$$\nabla \cdot (\alpha \rho U) = 0 \quad (19)$$

Momentum equation:

$$\begin{aligned} \frac{\partial(\alpha \vec{U}_R)}{\partial t} + \nabla \cdot (\alpha \vec{U}_R \vec{U}_I) - \nabla \cdot (\eta_{eff} \nabla \vec{U}_I) \\ = -\frac{d\Omega}{dt} \times \vec{r} - \vec{\Omega} \times \vec{U}_R \\ - \frac{\nabla p}{\rho} + F_s \end{aligned} \quad (20)$$

The \vec{U}_I is absolute velocity and \vec{U}_R is the relative velocity. If $\vec{\Omega}$ is zero, then $U_R = U_I$. Source term (F_s) in the equation (20) may be contemplated as the effect of the particle phase to the fluid phase.

Energy equation:

$$\frac{\partial(\alpha_1 T_1)}{\partial t} + \nabla \cdot (\alpha_1 T_1 U) = \nabla \cdot (\alpha_1 T_1 U) \quad (20)$$

$$\frac{\partial(\alpha_1 T_1)}{\partial t} + \nabla \cdot (\alpha_1 T_1 U) = \nabla \cdot (D_1 \nabla T_1) \quad (21)$$

The variation of the physical parameters such as viscosity, density, thermal conductivity, and heat capacity can be calculated by the following relationships:

When the temperature changes, the value of viscosities (μ), are varied, we have [38]:

$$\mu = 1.79 \exp\left(\frac{(-1230 - T_1)T_1}{36100 + 360T_1}\right) \quad (22)$$

Where μ is cP, T_1 is in °C, and the temperature range is between $0 < T_1 < 100$.

For density [39]:

$$\rho = 1258 - 0.654T_1 \quad (23)$$

The temperature range is $17 < T_1 < 83$.

For C_p we have [40]:

$$C_p = 90.983 + 0.4335T_1 \quad (24)$$

Where C_p and T are as J/mol.K and Kelvin, respectively.

Furthermore, for thermal conductivity, k , the following equation is applied [41]:

$$k = 0.00074 + 0.00000008T_1 \quad (25)$$

The unit of k is [cal.sec⁻¹.cm⁻². °C⁻¹.cm].

Now each of these variables is defined in the creatFields.H of OpenFOAM.

3. Simulation procedure

3.1. Mesh geometry

The computational regions were divided into several sub-sections to make the geometry. The unstructured tetrahedral mesh was employed for moving zones consist the tank volume, agitator, and hexahedral meshes that were applied for walls where they were stationary sections. The total number of cells was 235949. Figure 1 depicts the mesh view for the agitating apparatus. The finite volume procedure and the second-order modified algorithm were used to solve the Navier-Stokes equations. Figure 1 reveals a mesh picture of the agitator used in the mixing tank.

In order to create geometry, it is applied to the SnappyHex- Mesh tool. The file stl is created with the software Catia which is presented in Figure 2.

The mixing system may be divided into two parts: moving reference frames and static tank in Figure 3.

As it was portrayed in Figure 3, moving areas that are included the impeller and environment that it is sweeping by the impeller.

3.2. Solving strategies

The first step in problem-solving is solver selection. Therefore, the DPMFoam Lagrangian solver was employed in this work. The best solver is sensitive to the mesh. Mesh quality has an important impact on the rate of convergence (or non-convergence), accuracy solving, and time calculations.

3.2.1. Boundary conditions

The helical ribbon impeller is centered in a flat-bottomed cylindrical tank with diameter $T = 0.276$ m, and a liquid height, $H = 0.21$ m. The diameter and height of the impeller are $D = 0.255$ m, $h = 0.14$ m, respectively. The important dimensionless parameters governing the vessel were: $h/D = 0.549$, $w/D = 0.118$, and $T/D = 1.082$, where D , h , c , w , and T , are the ribbon outer diameter, ribbon

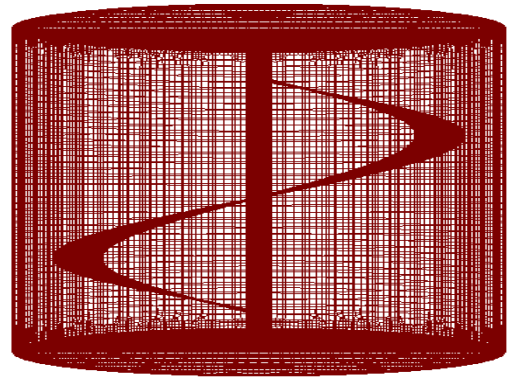


Figure 1. A mesh view of the tank and agitator.

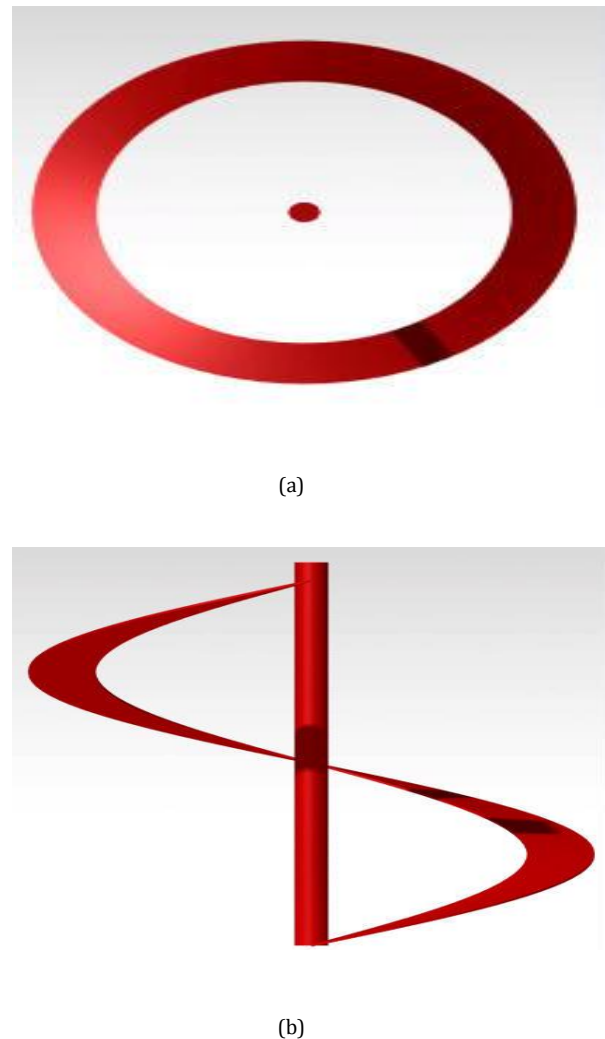


Figure 2. Impeller geometry from Catia, (a) top, (b) side view.

height, ribbon to wall clearance, ribbon width, and tank diameter, respectively.

Spherical particles with a diameter of 2.1 mm, density 2,500 kg/m³, and glycerin with a density of 1258 kg/m³ and the viscosity 1.41 Pa.s were applied as fluid in the tank. The roof of the vessel was closed by one polymer sheet. Moreover, the impeller rotational speed is 16 rpm. We

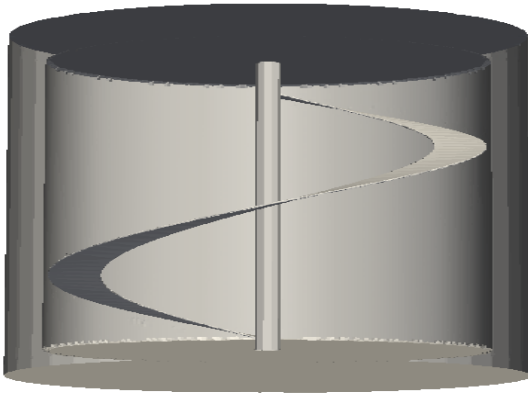


Figure 3. Specifying area of moving reference frame.

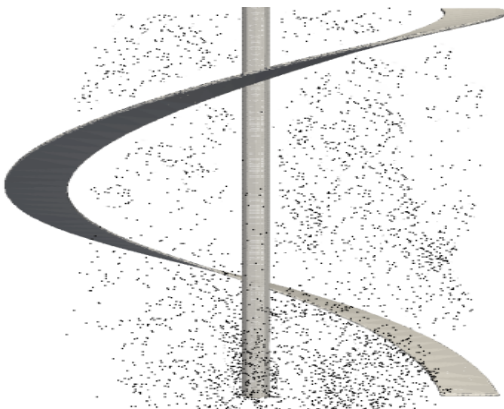


Figure 4. Distribution of concentration in the final time step.

assumed the temperature of the tank wall was kept at 400K, and inside the tank and impeller were set to 300K. The initial position of the particle was generated by Excel software in the form of random points. The solver would not start unless the points being set inside the computational domain. Further, clearance, which represents the distance of the impeller from the tank bottom, was set $c = 0.1$ [33-42].

Since for Newtonian liquids, any vortex reveals for revolution velocity less than 300 rpm [4,39], the free surface is defined as a symmetrical boundary condition for both Newtonian and non-Newtonian liquids where the normal velocity vector is zero and no velocity slip condition assumed for solid walls. For more information, see [4].

3.2.2. Validation

Flow patterns produced by helical ribbon impellers have been deliberated in some studies[4,38]. In spite of some impeller geometries, the primary circulation patterns are almost similar. Usually, the liquid between the agitator and the wall flows upwards, inwards along the surface. Further detailed information could be found in reference [4].

The distribution of concentration in the final time step is portrayed in Figure 4. This figure revealed that the final

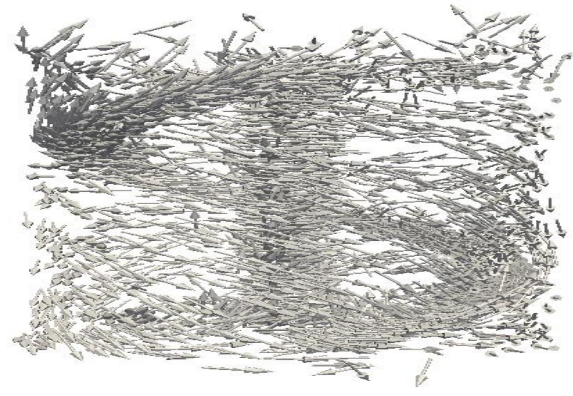


Figure 5. 3-D contour velocity.

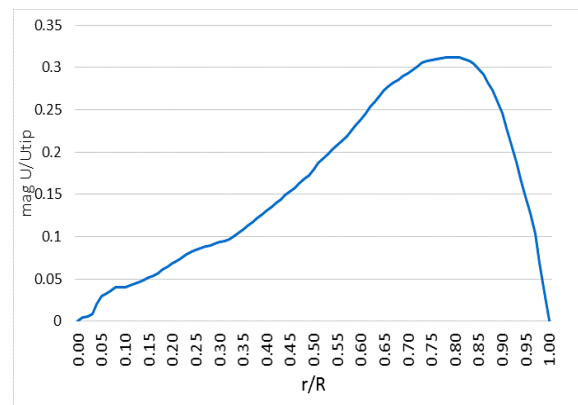


Figure 6. Dimensionless Velocity versus dimensionless radius.

time step is dispersed uniformly.

Furthermore, the 3-D contour velocity for the model is demonstrated in Figure 5. This figure displayed that the impeller has flow suction in the tank bottom and flow discharges in the upper section of the tank.

In addition, acquired velocity against the dimensionless radius are presented in Figure 6.

In the present model in order to make sure that the heat transfer is done correctly, two assumptions were considered: 1) The temperature of the outer wall of the tank which is associated with the environment should be 400 K, 2) The temperature of the inner wall of the tank and impeller should be kept at 300K for the first time step.

Figure 7 indicates the temperature distribution for the last time step. The temperature distribution is achieved as follows:

In order to acquire the heat flux according to the following equation, we considered:

$$Q = -k\nabla T_1 \quad (26)$$

Applying the command `foamCalc magGrad T` and also `plotOverLine` provided the variation of temperature gradient and heat flux, which is indicated in Figure 8.

Considering Figure 8, we find that the value of $\text{grad } T$ (heat flux) is enhanced from the beginning of the impeller shaft to the sidewall of the tank. Moreover, for the

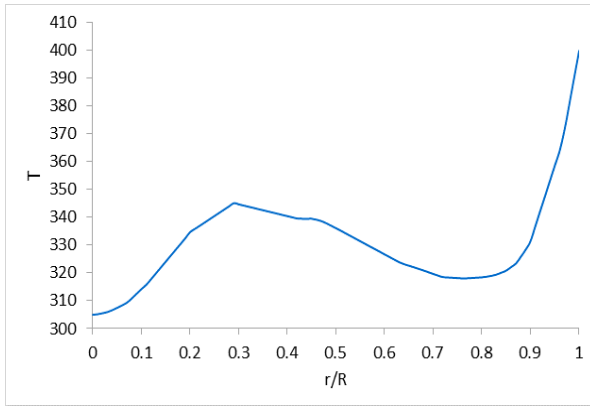


Figure 7. Temperature distribution.

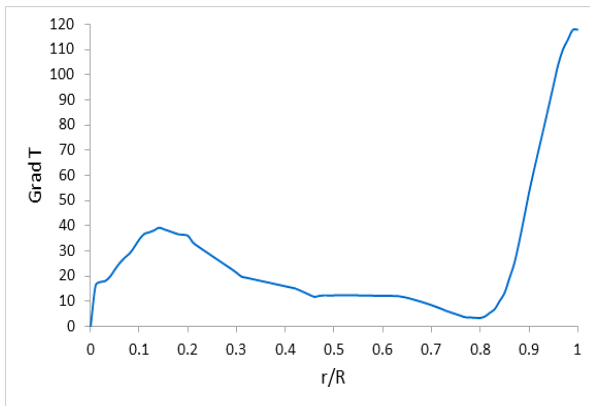


Figure 8. The amount of Grad T relative to the radius.

calculation Nusselt dimensionless number (Figure 9) that is the ratio of convective to conduction heat transfer,[24]:

$$Nu = \frac{\nabla T_1}{(T_1 - T_{ref})} 2R \quad (27)$$

In this case, the characteristic length is the radius. Moreover, the reference temperature is ambient.

Furthermore, Nusselt number variations with respect to the z-axis of the tank wall are shown in Figure 10.

In which, the characteristic length is the radius, and the reference temperature is the ambient one. Many of the equations acquired by the researchers are devoted to single-phase mode. Hamidi and Postchi [43] were obtained the relationship for the Nusselt number for a three-phase mixture.

$$Nu = 1.2467Re^{0.896}Pr^{0.33} \left(\left(\frac{\mu}{\mu_w} \right)^{0.14} \right) \left(\left(\frac{d_p}{D} \right)^{0.238} \right) \left(\left(\frac{V_g}{ND} \right)^{0.393} \right) \quad (28)$$

The exact form of the relationship in Eq. (28) will be established by inspecting the contribution of each group separately, resulting in simple forms for the functional dependencies. Of course, in practice, it is desirable to avoid operating conditions that give rise to steep temperature gradients; it would, therefore, be beneficial in order to have predictive equations for the onset of such conditions.

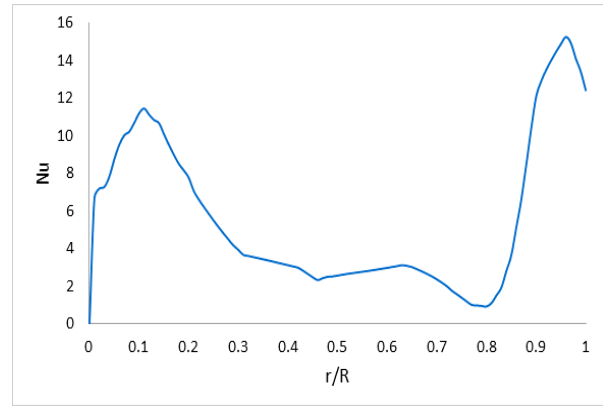


Figure 9. Variations of Nusselt number relative to dimensionless radius. ($h/D = 0.549$, $w/D = 0.118$, and $T/D = 1.082$, $Re < 300$, $Pr < 1000$)

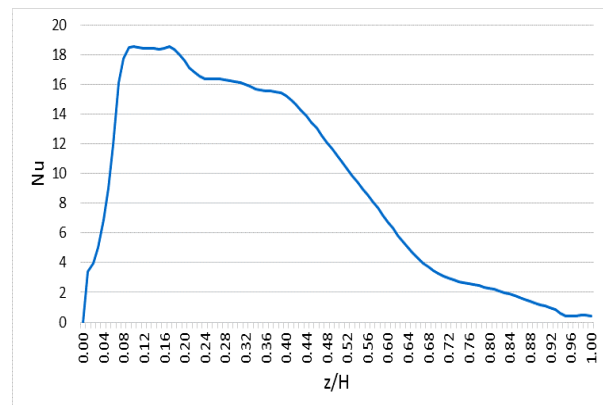


Figure 10. Nusselt number variations relative to the z - Axis in the tank wall. ($H = 0.21m$, $h/D = 0.549$, $w/D = 0.118$, and $T/D = 1.082$, $Re < 300$).

In order to provide a new correlation between Nu and Re numbers, one may be applied Nu at three vertical points in the mixing tank [24, 33, 42-44] as the data of Table 2.

Applying the above data, variations of Nusselt against Reynolds numbers are portrayed in Figure 11.

In consonance with the figure above and compare it with the research work of Rai and Devotta [44], one may be observed that the trend will be confirmed as well. As a result of small changes in the geometry of the simulation system and applying Matlab software, the following correlation is yield:

$$Nu = 0.37Re^{0.92}Pr^{0.333}Vi^{0.14} \quad (29)$$

It is noteworthy to mention that due to changes in the physical properties of the fluid versus temperature and also the existence of solid particles and its unpredictable behavior, Nusselt values vary in each region. In Table 3, we see three relationships acquired for the Nusselt number. The viscosity ratio (Vi) and Pr number are nearly similar to the References [33, 40, 42, 43]. This may have arisen from the suitable selection from the low concentration of solid particles in this work. On the other hand, the physical properties of two-phase very close to one in this work.

Table 2. Nusselt and Reynolds values at three levels of the tank.

Vertical distance from bottom of mixing tank	Nu	Re
0.131474	16.0842	3.43405
0.132934	14.3348	3.10007
0.134395	14.158	2.75458

3.3. The effect of solid particles on the temperature profile

The temperature profiles for one and two-phase flow in the tank are displayed in Figure 12. This figure revealed that the level of the temperature is higher for one phase. Then

the level of the temperature is higher for one phase. Then again, the particles may help to the heat transfer rate enhancement in the fluid of the tank.

Conclusion

The two-phase fluid, including glycerine and solid particles, was mixed by the helical impeller. This mixing process was simulated by applying the Catia and OpenFOAM. Velocity Contour, solid particle profiles, and temperature distribution in the tank are studied. Following results are acquired:

1. Total velocity contour for three-dimensional simulation in the tank indicated that the impeller had pumped the fluid from bottom to upper section of the tank.
2. The results suggested that solid particles properly had distributed in the mixing tank.
3. It was observed that the temperature gradient and heat flux are increased from the impeller shaft to the

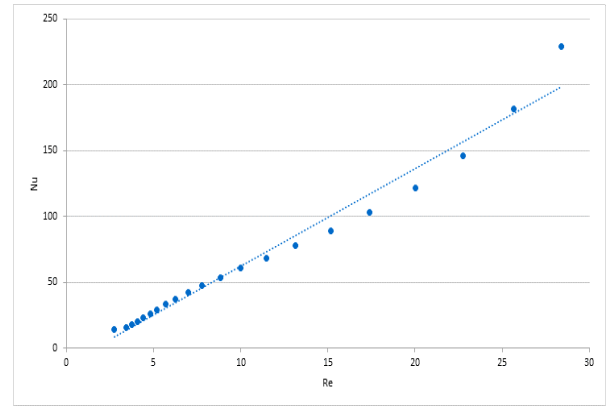


Figure 11. Variations of Nusselt relative to the Reynolds numbers. ($H = 0.21\text{m}$, $h/D = 0.549$, $w/D = 0.118$, and $T/D = 1.082$, $Pr < 1000$)

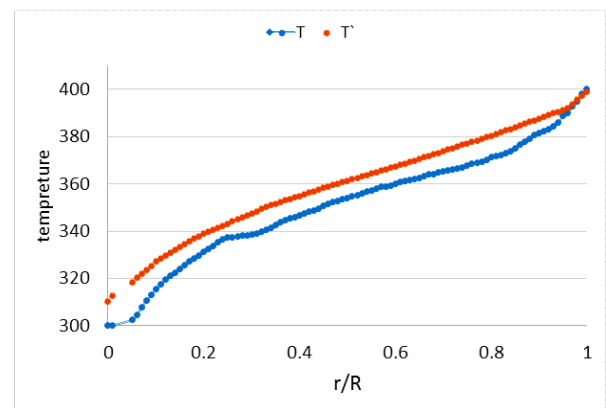


Figure 12. A comparison of the temperature distribution, T (two-phase), and T' (single-phase).

walls of the mixing tank.

4. A new correlation for the Nusselt number as a function of Re, Pr, and Vi in the laminar region are presented ($Re < 10$).

Table 3. A Comparison of Nusselt number in the literature.

Researchers	Nu
Ayazi shamlou, single phase [33]	$Nu = 0.568 Re^{0.23} Pr^{0.23} n_b^{0.23} \left(\frac{C}{T}\right)^{-0.54}$
Hamidi and Postchi, Three-phase [43]	$Nu = 1.2467 Re^{0.896} Pr^{0.33} \left(\left(\frac{\mu}{\mu_w}\right)^{0.14}\right) \left(\left(\frac{d_p}{D}\right)^{0.238}\right) \left(\left(\frac{V_g}{ND}\right)^{0.393}\right)$
Ishibashi et al., single-phase [42]	$Nu = 2.0 Re^{0.33} Pr^{0.33} Vf^{0.14}$
Negata et al., single-phase [32]	$Nu = 0.42 Re^{0.67} Pr^{0.33} Vf^{0.14}$
In this work, two-phase	$Nu = 0.37 Re^{0.92} Pr^{0.333} Vf^{0.14}$

Nomenclature

c	clearance
C_p	heat capacity
C_s	saffman coefficient
d, d_p	particle diameter
D	impeller diameter
D_1	diffusion coefficient
$D u_f / D t$	total velocity derivative
F	force
F_D	drag force
F_{gr}	gravity force
F_p	particle force
F_s	saffman force
g	gravity constant
h_j	heat transfer coefficient
k	thermal conductivity
mp	particle mass
nb	number of blades
N	rotational speed of the impeller
NC	critical impeller speed
Nu	Nusselt number
p	impeller pitch
∇P	pressure gradient
Q	overall heat transfer rate
Pr	Prandtl number
Re	Reynolds number
t	contact time
T	tank diameter
T1	temperature
Tb	bulk temperature
Tref	reference temperature
Tw	wall temperature
Uf	fluid velocity
Up	particle velocity
UR	relative velocity
UI	absolute velocity
Vi	viscosity ratio
Vp	particles velocity
w	impeller width
Xp	local coordinate

Greek letter

α	constant
α_1	diffusivity (= $k/\rho T_1$)
η_{eff}	effective viscosity
ρ	density
ρ_p	particle density
ρ_f	fluid density
μ	viscosity
μ_f	fluid viscosity
μ_w	water viscosity
ω	angular velocity

Ω rotation velocity

Acknowledgements

We are so grateful for the financial and encouragement support provided by the Research Vice Presidency of Semnan University.

References

- [1] Brucato, A., Ciofalo, M., Grisafi, F., and Micale, G., (1988), Numerical Prediction of Flow Fields in Baffled Stirred Vessels: a Comparison of Alternative Modelling Approaches, *Chem. Eng. Sci.*, 53, 3653–3684.
- [2] Mavros, P., (2001), Flow Visualization in Stirred Vessels a Review of Experimental Techniques, *Trans IChemE*, 79, Part A, 113–127.
- [3] Tsui, Y., Hu, Y., (2011), Flow characteristics in mixers agitated by helical ribbon blade impeller, *Application of Computational Fluid Mechanics*. 5, 416-429.
- [4] Sanaie-Moghadam, M., Jahangiri, M., and Hormoszi, F., (2015), Determination of stationary region boundary in multiple reference frames method in a mixing system agitated by Helical Ribbon Impeller using CFD, *Heat and Mass Transfer Research. J.*, 2, 31-37.
- [5] Iranshahi, A., Heniche, M., Bertrand, F. and Tanguy, P. A., (2006), Numerical investigation of the mixing efficiency of the Ekato Paravisc impeller, *Chem. Eng. Sci.*, 61(8), 2609-2617.
- [6] Aubin, J., Naude, I., Xuereb, C., Bertrand, J., (2000), Blending of Newtonian and Shear-Thinning Fluids in a Tank Stirred with a Helical Screw Agitator, *ChERD Trans. IChemE.*, 78, 1105-1114.
- [7] Aubin, J., Naude, I., Xuereb, C., (2006), Design of Multiple Impeller Stirred Tanks for the Mixing of Highly Viscous Fluids Using CFD, *Chem. Eng. Sci.*, 61, 2913-2920.
- [8] Letellier, B., Xuereb, C., Swaels, P., Hobbes, P., Bertrand, J., (2002), Scale-up in laminar and transient regimes of a multi-stage stirrer, a CFD approach, *Chem. Eng. Sci.*, 57, 4617-4632.
- [9] Sanjuan-Galindo, R., Heniche, M., Ascanio, G., Tanguy, P.A., (2011), CFD investigation of new helical ribbon mixers bottom shapes to improve pumping, *Asia-Pac. J. Chem. Eng.*, 6, 181–193.
- [10] Ameer, H., Bouzit, M., Helmaoui, M., (2011), Numerical study of fluid and power consumption in a stirred vessel with a Scsbs 6SRGT impeller, *Chem. Process Eng.*, 32, 351-366.

- [11] Ameer, H., Bouzit, M., (2012), Agitation of Yield Stress Fluids by Two-Blade Impellers, *Canadian J. Chem. Eng. Technol.*, 3, 93-99.
- [12] Luo, J.Y., Issa R. I., Gosman, A.D., (1993), Prediction of impeller induced flows in mixing vessels using multiple frames of reference, *Proceeding Institution Chem. Eng.* 136, 549-556.
- [13] Ng, K., Fentiman, N. J., Lee, K.C., and Yianneskis, M., (1998), Assessment of Sliding Mesh CFD Predictions and LDA Measurements of the Flow in a Tank Stirred by a Rushton Impeller, *Trans. IChemE*, 76, 737-747.
- [14] Montante, G., Lee, K.C., Brucato, A., and Yianneskis, M., (2001), Numerical Simulations of the Dependency of Flow Pattern on Impeller Clearance in Stirred Vessels, *Diffusion in a Particle, AIChE*, 45 (56) 3751-3770.
- [15] Pérez-Terrazas, J. E., Ibarra-Junquera, V. and Rosu, H. C., (2008), Cellular automata modeling of continuous stirred tank reactors, *Korean. J. Chem. Eng.*, 25, 461.
- [16] Um, B. H. and Hanley, T. R., (2008), A CFD model for predicting the flow patterns of viscous fluids in a bioreactor under various operating conditions, *Korean. J. Chem. Eng.*, 25, 1094.
- [17] Aubin, J. and Xuereb, C., (2006), Design of multiple impeller stirred tanks for the mixing of highly viscous fluids using CFD. *Chem. Eng. Sci.*, 61, 2913-2920.
- [18] Jahangiri, M., (2007), Velocity distribution of helical ribbon impeller in mixing of polymeric liquids in the transition region, *Iranian Polymer*, 16, 731-739.
- [19] Jahangiri, M., (2006), Fluctuation velocity for non-Newtonian liquid in mixing tank by Rushton turbine in the transition region, *Iranian Polymer J.*, 15(4) 285-290.
- [20] Jahangiri, M., (2008), Shear Rates in Mixing of Viscoelastic Fluids by Helical Ribbon Impeller, *Iranian Polymer J.*, 17(11)831-841.
- [21] Jahangiri, M., (2005), An LDA Study of the Rushton Turbine Velocity Profile for Mixing of Polymeric Liquids, *Iranian Polymer J.*, 14(6)521-530.
- [22] Aminian, A. Jahangiri, M., (2014), Predicting the Velocity Distribution of Rushton Turbine Impeller in Mixing of Polymeric Liquids Using Fuzzy Neural Network Model, *Korean J. Chem. Eng.*, 31(5) 772-779.
- [23] Liu, Li., (2014), Computational fluid dynamics modelling of complex fluid flow in stirred vessels, Ph.D. thesis, University of Birmingham.
- [24] Rosa V. S., Júnior, D. M. (2019), Review Heat Transfer of Non-Newtonian Fluids in Agitated Tanks, *Heat and Mass Transfer, Advances in Science and Technology Applications*, DOI: <http://dx.doi.org/10.5772/intechopen.85254>
- [25] Coyle C. K., Hirschland, H. E., Michel, B.J., Oldshue J.Y. (1970), Heat transfer to jackets with close clearance impellers in viscous liquids, *Can. J. Chem. Eng.*, 48, 275-278.
- [26] Harriott P., (1959), Heat transfer in scraped-surface exchangers. *Chem. Engng. Prog.*, 54, 137-139.
- [27] Latinen A. G., (1959), Correlation of scraped film heat transfer in the Votator, *Chem. Engng Sci.* 9(4) 263-266.
- [28] Rautenbach R. and Bollenrath F. M., (1979), *Fluid Mechanics and Heat Transfer With Non-Newtonian Liquids in Mechanically Agitated Vessels*, *German chem. Engng*, 2 18-24.
- [29] Chilton H. and Drew B., (1944), Heat transfer coefficients in agitated vessels, *Int. Engng Chem.* 36 510-516.
- [30] Kapustin A. S., (1963), Investigations of heat exchange in agitated vessels working, *Int. Chem. Engng*, 4, 514.
- [31] Seider, E.N., Tate, G.E., (1936), Heat transfer and pressure drop of liquid in tubes, *Ind. Eng. Chem.* 28 1429-1434.
- [32] Negata, S., Nishikawa, M. and Kayama, T., (1972), Heat transfer to vessel with impeller for highly viscous fluids, *J. Chem. Eng. Jap.* 5 83-85.
- [33] Ayazi S., P., Edwards, M. F., (1986), Heat transfer to viscous Newtonian and non-Newtonian fluids for helical ribbon mixers, *Chem. Eng. Sci.*, 41(8) 1957-1967.
- [34] Lillo G., Mastrullo R., Mauro A.W., Viscito L., (2019), Flow boiling of R32 in a horizontal stainless steel tube with 6.00 mm ID. Experiments, assessment of correlations and comparison with refrigerant R410A, *Inter. J. Refrigeration* 97,143-156.
- [35] Mizushima, T. R., Kagaku K. (1970), Heat transfer under solidification of liquid on agitated vessel wall, *J Chem., Eng. Jap.* 34 1205.
- [36] Mitsuiishi, N. and Miyairi Y., (1973), Heat transfer to non-Newtonian fluids in an agitated vessel, *J. Chem. Eng. Jap.* 6 415-420.
- [37] Nishikawa, M. (1972), Heat transfer in agitated vessels with special types of impellers, *J. Chem. Eng. Jap.* 5 83.
- [38] Uhl, V. W., (1955), Heat transfer to viscous materials in jacketed agitated kettles, *Chem. Eng. Symp.* 51 93-108.
- [39] Adams L.W., (2009) "Experimental and computational study of non-Turbulent flow regimes and cavern formation of non-

- Newtonian fluids in a stirred tank,' PhD thesis, Birmingham, B15 2TT.
- [40] Uhl, V. W. and Voznick H. P., (1960), Heat transfer in mechanically agitated gas-liquid systems, *Chem. Eng. Prog.* 56 72-77.
- [41] Rahimi, M., Kakekhani, A., AbdulazizAlsairafi, A., (2010), Experimental and computational fluid dynamic (CFD) studies on mixing characteristics of a modified helical ribbon impeller, *Korean J. Chem. Eng.* 27 pp.1150-1158.
- [42] Ishibashi, K., Yamanaka A., Mitsuishi N., (1979), Heat transfer in agitated vessels with special types of impellers, *J. Chem. Eng. Japan*, 12(3)230-235.
- [43] Hamidi, A.A and Postchi, A.A. (2002), determine the heat transfer coefficient of the three-phase mixture in the tank walls equipped with a mechanical stirrer with non-standard blade, *J. Technology Faculty of Tehran*, 37(4) 347-358.
- [44] Rai, C.L., Devotta, I., Rao, P.G., (2000), Heat transfer to viscous Newtonian and non-Newtonian fluids using helical ribbon agitator, *Chem. Eng. J.*, 79 73-77.